An overview and some new developments in the statistical analysis of PET and fMRI data

K.J. Worsley

March 7, 1997

Department of Mathematics and Statistics, McGill University, 805 Sherbrooke St. West, Montreal, Québec, Canada H3A 2K6, and McConnell Brain Imaging Centre, Montreal Neurological Institute, 3801 University Street, Montreal, Québec, Canada H3A 2B4

The first part of this paper gives an overview of a simplified approach to the statistical analysis of PET and fMRI data, including new developments and future directions. The second part outlines a new method, based on multivariate linear models (MLM), for characterising the response in PET and fMRI data, which overcomes some of the drawbacks of current methods such as SSM, SVD, PLS and CVA.

Running title: An overview of statistical analysis

Addresses of corresponding author:
e-mail: worsley@math.mcgill.ca
web: http://www.math.mcgill.ca/∼keith
ph: 1-514-398-3842
fax: 1-514-398-3899.

1 Overview

The first part of this paper is an attempt to give a unified statistical analysis suitable for all types of PET and fMRI data. It is not intended as an exhaustive compilation of all statistical methods. Some of the more specialised methodologies, taylored to one type of data, may have been missed out, while others may be over-emphasised. Only some of the more recent references are given and many other contributions have been omitted to simplify the presentation.

Table 1 is an attempt to capture this as a single schematic representation. In the text that follows, **bold face** refers to the text in Table 1. At the top, the goals of image analysis are divided into **functional changes**, that is, changes in brain activity, and **structural changes**, changes in neuroanatomy; this latter aspect is very recent. Functional changes are divided into three methodologies: **PET CBF** studies using O^{15} labelled water; **PET kinetics** (Malizia *et al.,* 1995), where the goal is to study changes in uptake curves or rate constants; and **fMRI**. Changes in a structure such as grey or white matter, a gyrus or a sulcus, can be detected using three different methodologies: **segemented MR** images of the structure, where each voxel records the presence (1) or absence (0) of the structure (Wright *et al.,* 1995); **surface extraction** using a new automated method (MacDonald *et al.,* 1996; Worsley *et al.,* 1996c; Thompson *et al.,* 1996; Zilles *et al.,* 1996); and **non-linear deformations** required to move the structure to an atlas or standardised structure (Collins *et al.,* 1995; Kjems *et al.,* 1996).

Images derived from these different techniques can all be treated in a similar way, though of course the details differ greatly from one type of data to another. Broadly speaking, the signal to noise ratio is very small and so the signal is enhanced by two methods. The first involves **spatial smoothing** of the images, with the amount of smoothing chosen to match the signal to be detected. Trying all possible smoothing filter widths adds an extra **scale space** dimension to the data (Poline & Mazoyer 1994; Worsley *et al.,* 1996b). The second involves simply repeating the experiment either on different subjects (which requires careful image registration), or on different scans within the same subject. The result is a set of **dependent variables**, $\mathbf{Y}$, one for each voxel of the images.

These are related to a set of **predictor variables**, $\mathbf{X}$, which are measured on each image. These include **factors** such as **tasks** (baseline, stimulus) or **groups** of subjects (cases, controls), leading to **ANOVA** type models, or continuous **variates**, leading to **ANCOVA** type models, with possible **quadratic** or **polynomial** effects in these variates (Büchel *et al.,* 1996). Replacing the variate by the image values at a single voxel gives an analysis of the **covarying voxels**.

Relationships between $\mathbf{Y}$ and $\mathbf{X}$ can be studied using **exploratory** methods such as **SVD** (Singular Value Decomposition; Friston *et al.,* 1993), **SSM** (Scaled Subprofile Models; Strother *et al.,* 1995), **PLS** (Partial Least Squares, McIntosh *et al.,* 1996), **SVD-CVA** (SVD followed by Canonical Variates Analysis; Friston *et al.,* 1995c, 1996a), or **MLM** (Multivariate Linear Models; Worsley *et al.,* 1997). The last method is discussed in more detail in the next section. These methods can be extremely useful at suggesting relationships or generating hypotheses that might be confirmed by further analysis. These methods also test for a global relationship between $\mathbf{Y}$ and $\mathbf{X}$, but it is not possible to make local inference about changes at the voxel level. A second broad class of methods looks at **connectivity** between pre-defined brain regions and their relationships to $\mathbf{X}$: **Path Analysis** and **Structural Equations** (Horowitz *et al.,* 1996). It must be stressed that connectivity here means correlations between

voxel, VOI and **X** variables, which does not necessarily indicate connectivity at the neuronal level.

The most widely used tool for assessing relationships between **X** and **Y**, rather than exploring them, is the **linear model** (Friston *et al.,* 1995a; Worsley and Friston, 1995). Essentially the straightforward linear model involving **X** is applied separately to each voxel of **Y**. Some pooling of error sum of squares over voxels may increase the error degrees of freedom and hence the sensitivity. This methodology has been found to be sufficiently flexible to treat image data from all the above six sources; the only slight generalisation required is a multivariate linear model for the three components of deformations data, and a generalised linear model for binary data. Lange and Zeger (1997) develop a much more sophisticated model for fMRI data that incorporates spatially varying hemodynamic response.

The scientific question of interest can usually be reduced to testing for one or more coefficients of the linear model at each voxel. this leads to a **statistical map** (SPM) of test statistics, usually of the form of the coefficient **b** divided by an estimated standard deviation **Sd**. Inference about this image can be made at four levels: the **voxel level**, using a test based on the height of **local maxima** (Friston *et al.,* 1991; Worsley *et al.,* 1992; Worsley *et al.,* 1996a); the **cluster level**, using a test based on the **spatial extent** of contiguous voxels above a threshold (Friston *et al.,* 1994); a combination of these (Poline *et al.,* 1997); the **set level**, using a test based on the **total clusters** above a threshold (Friston *et al.,* 1996b); or the **global level**, using a test based on the **total voxels** above a threshold or **sum of squares** of all voxel values (Worsley *et al.,* 1995). **Validity** of these tests is based on **random field theory** (Adler, 1981; Worsley 1996), provided certain assumptions about the Gaussian distribution of the images and their stationarity are met. If this is doubtful, then **non-parametric** and **randomisation** methods are available (Holmes *et al.,* 1996) at the expense of extra computation.

The details of the use of these procedures can be quite different for different types of data. For example, fMRI data shows marked temporal correlation that requires modification to the least squares theory for linear models (Worsley & Friston, 1995); the same may also be true of PET kinetic data. Non-stationary voxel standard deviation is a characteristic of fMRI data and all three forms of structural data. In addition, the structural data has non-stationary smoothness. All of these are the subject of on-going research.

2 Characterizing the response of fMRI data using multivariate linear models

The aim of methods of characterizing global brain response is two-fold. The first is to provide a sensitive global test of non-focal activation in blood flow images in response to a set of predictor variables (predictors) measured for each scan. The second is to capture, summarise, or explain, the correlation between predictors and voxel blood flows by a small number of latent variables, one set for predictors and one set for voxels. These latent variables take the form of *weights*; if the characterization is successful, then the weighted average of the voxel blood flows should be highly correlated with the corresponding weighted average of the predictors, over scans. This is summarised in Table 2, in which **X** and **Y** represent the scans $\times$ predictors and scans $\times$ voxel blood flow matrices, respectively, possibly standardised to have zero mean and unit standard deviaiton. Their complex covariance structure is $\mathbf{X}'\mathbf{Y}$. **U** and **V** are the (orthonormal) latent variables $\times$ predictors and latent variables $\times$ voxels

matrices, respectively. The weighted averages, or predicted and observed temporal responses, are $\mathbf{XU}'$ and $\mathbf{YV}'$ respectively. Their simpler covariance structure is the diagonal matrix of latent roots $\mathbf{\Lambda}$. This is achieved by choosing $\mathbf{U}$ and $\mathbf{V}$ so that $\mathbf{U}'\mathbf{\Lambda}\mathbf{V}$ approximates $\mathbf{X}'\mathbf{Y}$.

Current methods for carrying this out are summarised in Table 2. These methods all have some drawbacks: SSM and straightforward SVD only model the responses; orthonormalised PLS takes into account correlation between the predictors $\mathbf{X}$, but the inference, based on randomization, is not valid for temporally correlated scans such as fMRI data; classical CVA takes into account correlations betwen both responses and predictors, but this is not possible if, as is usually the case, there are more voxels than images; a preliminary SVD, followed by CVA overcomes this but again the inference is not valid for temporally correlated data.

The last method, based on multivariate linear models, attempts to overcome these drawbacks (Worsley *et al.,* 1997). It approximates the least squares regression coefficients $\mathbf{b}$ standardised by its variance, which depends on the variance of the scans, $\mathbf{\Sigma}$. For PET data with uncorrelated scans, this is simply an identity matrix; for fMRI data, it can be modelled by assuming that the temporal correlations are generated by white noise convolved with the (known) hemodynamic response function. Inference for the number of canonical variates, or non-unit latent roots, is corrected for temporal and spatial correlation as follows. The diagonal matrix of latent roots is

$$\mathbf{\Lambda} = \mathrm{diag}(\lambda_1, \ldots, \lambda_h).$$

Tests for their significance is based on partial averages of the latent roots

$$S_q = \frac{\mathrm{Average}(\lambda_{q+1}^2, \ldots, \lambda_h^2)}{\#\mathrm{voxels}}.$$

Their effective spatial degrees of freedom is

$$d = \mathrm{RESELS}(4 \log_e 2/\pi)^{D/2}.$$

They can be converted into F-statistics F_q with ν_1, ν_2 degrees of freedom where

$$\begin{aligned} \nu &= \text{residual degrees of freedom}, \\ \nu_1 &= d(h-q), \\ \nu_2 &= d\nu - \frac{(d-1)(4(h-q)+2\nu)}{h-q+2}, \end{aligned}$$

$$F_q = \frac{\nu - 2}{\nu} \frac{\nu_2}{\nu_2 - 2} S_q.$$

Starting with $q = 0$, F_0 tests for any non-unit latent roots, that is, for any effect of predictors on the images. If this is rejected, F_1 tests for non-unity of all latent roots except the first; if this is accepted, there is just one latent root, but if this is rejected, then F_2 tests for non-unity of all latent roots except the first two. This is repeated until F_q is accepted, indicating that there are just q non-unit latent roots and the rest are unity. We would then conclude that the data can be charcterised by just q latent variables.

This method has been applied to the data of Friston *et al.* (1995c) in which a set of basis functions were used to capture a differential response to a stimulus under three different test conditions. Just one latent root was significant. The corresponding temporal response (eigenvector) suggested a difference between the onset of the response to two of the three

stimuli, and the corresponding spatial response (eigenimage) agreed quite closely with the SPM used to detect this difference in an earlier paper Friston *et al.* (1995b) that analysed the same data by a straightforward linear model. Details are reported in Worsley *et al.* (1997).

References

Adler, R.J. 1981. *The Geometry of Random Fields.* Wiley, New York.

Büchel, C., Wise, R.J.S., Mummery, C.J., Poline, J-B., and Friston, K.J. 1996. Non-linear regression in parametric activation studies. *NeuroImage*, **4:**60-66.

Collins, D.L., Holmes, C.J., Peters, T.M., and Evans, A.C. 1995. Automatic 3-D model-based neuroanatomical segmentation. *Human Brain Mapping*, **3:**190-208.

Friston, K.J., Frith, C.D., Liddle, P.F., and Frackowiak, R.S.J. 1991. Comparing functional (PET) images: The assessment of significant change, *Journal of Cerebral Blood Flow and Metabolism*, **11:**690-699.

Friston, K.J., Frith, C.D., Liddle, P.F., and Frackowiak, R.S.J. 1993. Functional connectivity: The principal-component analysis of large (PET) data sets. *Journal of Cerebral Blood Flow and Metabolism*, **13:**5-14

Friston, K.J., Worsley, K.J., Frackowiak, R.S.J., Mazziotta, J.C., and Evans, A.C. 1994. Assessing the significance of focal activations using their spatial extent. *Human Brain Mapping*, **1:**214-220.

Friston, K.J., Holmes, A.P., Worsley, K.J., Poline, J-B., Frith, C.D., and Frackowiak, R.S.J. 1995a. Statistical parametric maps in functional imaging: A general linear approach. *Human Brain Mapping*, **2:**189-210.

Friston, K.J., Frith, C.D., Turner, R., and Frackowiak, R.S.J. 1995b. Characterizing evoked hemodynamics with fMRI. *NeuroImage*, **2:**157-165.

Friston, K.J., Frith, C.D., Frackowiak R.S.J., and Turner, R. 1995c. Characterizing dynamic brain responses with fMRI: A multivariate approach. *NeuroImage*, **2:**166-172.

Friston, K.J., Poline, J-B., Holmes, A.P., Frith, C.D., and Frackowiak, R.S.J. 1996a. A multivariate analysis of PET activation studies. *Human Brain Mapping*, **4:**140-151.

Friston, K.J., Holmes, A.P., Poline, J-B., Price, C.J., and Frith, C.D. 1996b. Detecting activations in PET and fMRI: Levels of inference and power. *NeuroImage*, **4:**223-235.

Holmes, A.P., Blair, R.C., Watson, J.D.G., Ford, I. 1996. Nonparametric analysis of statistic images from functional mapping experiments. *Journal of Cerebral Blood Flow and Metabolism*, **16:**7-22.

Horowitz, B., Grady, C.L., Mentis, M.J., Pietrini, P., Ungerleider, L.G., Rapoport, S.I., and Haxby, J.V. 1996. Brain functional connectivity changes as task difficulty is altered. *NeuroImage*, **3:**S248.

Kjems, U., Chen, C.T., Strother, S.C., Hansen, L.K., Anderson, J.R., Law, I., Paulson, O.B., Kanno, I., and Rottenberg, D.A. 1996. Revealing structural effects in functional imaging with anatomical warps. *NeuroImage*, **3:**S137.

Lange, N., and Zeger, S.L. 1997. Non-linear Fourier time series analysis for human brain mapping by functional magnetic resonance imaging (with Discussion). *Journal of the Royal Statistical Society, Series C (Applied Statistics)*, **14:**1-29.

MacDonald, D., Worsley, K.J., Avis, D. and Evans, A.C. 1996. Surface segmentation and matching by 3D deformation. *NeuroImage*, **3:**S253.

Malizia, A.L., Friston, K.J., Cunningham, V.J., Wilson, S., Jones, T., and Nutt, D.J. 1995. The analysis of brain PET radioligand displacement studies. *NeuroImage*, **2:**S52.

McIntosh, A.R., Bookstein, F.L., Haxby, J.V., and Grady, C.L. 1996. Spatial pattern analysis of functional brain images using Partial Least Squares. *NeuroImage*, **3:**143-157.

Poline J.B., and Mazoyer B.M. 1994. Enhanced detection in brain activation maps using a multifiltering approach. *Journal of Cerebral Blood Flow and Metabolism*, **14:**639-42.

Poline, J-B., Worsley, K.J., Evans, A.C., and Friston, K.J. 1997. Combining spatial extent and peak intensity to test for activations in functional imaging. *NeuroImage*, **5:**83-96.

Strother, S.C., Anderson, J.R., Schaper, K.A., Sidtis, J.J., Liow, J.S., Woods, R.P., Rottenberg, D.A. 1995. Principal component analysis and the scaled subprofile model compared to intersubject averaging and statistical parametric mapping: I. "Functional connectivity" of the human motor system studied with O^{15}water PET. *Journal of Cerebral Blood Flow and Metabolism*, **15:**738-753.

Thompson, P.M., Schwartz, C., and Toga, A.W. 1996. High-resolution random mesh algorithms for creating a probabilistic 3D surface atlas of the human brain. *NeuroImage*, **3:**19-34.

Worsley, K.J., Evans, A.C., Marrett, S., and Neelin, P. 1992. A three-dimensional statistical analysis for CBF activation studies in human brain. *Journal of Cerebral Blood Flow and Metabolism*, **12:**900-918.

Worsley, K.J.,, and Friston, K.J. 1995. Analysis of fMRI time-series revisited - again. *NeuroImage*, **2:**173-181.

Worsley, K.J., Poline, J-B., Vandal, A.C.,, and Friston, K.J. 1995. Tests for distributed, non-focal brain activations. *NeuroImage*, **2:**183-194.

Worsley, K.J., Marrett, S., Neelin, P., Vandal, A.C., Friston, K.J., and Evans, A.C. 1996a. A unified statistical approach for determining significant signals in images of cerebral activation. *Human Brain Mapping*, **4:**58-73.

Worsley, K.J., Marrett, S., Neelin, P.,, and Evans, A.C. 1996b. Searching scale space for activation in PET images. *Human Brain Mapping*, **4:**74-90.

Worsley, K.J., MacDonald, D., Cao, J., Shafie, Kh., and Evans, A.C. 1996c. Statistical analysis of cortical surfaces. *NeuroImage*, **3:**S108.

Worsley, K.J. 1996. The geometry of random images. *Chance*, **9(1):**27-40.

Worsley, K.J., Poline, J-B., Friston, K.J., and Evans, A.C. 1997. Characterizing the response of fMRI data using multivariate linear models *NeuroImage*, submitted.

Wright, I.C., McGuire, P.K., Poline, J-B., Travere, J.M., Murray, R.M., Frith, C.D., Frackowiak, R.S.J., and Friston, K.J. 1995. A voxel-based method for the statistical analysis of gray and white matter density applied to schizophrenia. *NeuroImage*, **2:**244-252.

Zilles, K., Falkal, P., Schormann, T., Steinmetz, H., and Palermo-Gallagher, N. 1996. Cortical surface in schizophrenic patients and controls: MRI, 3-D reconstruction and in vivo morphometry. *NeuroImage*, **3:**S525.

Table 1: Outline of Statistical Analysis

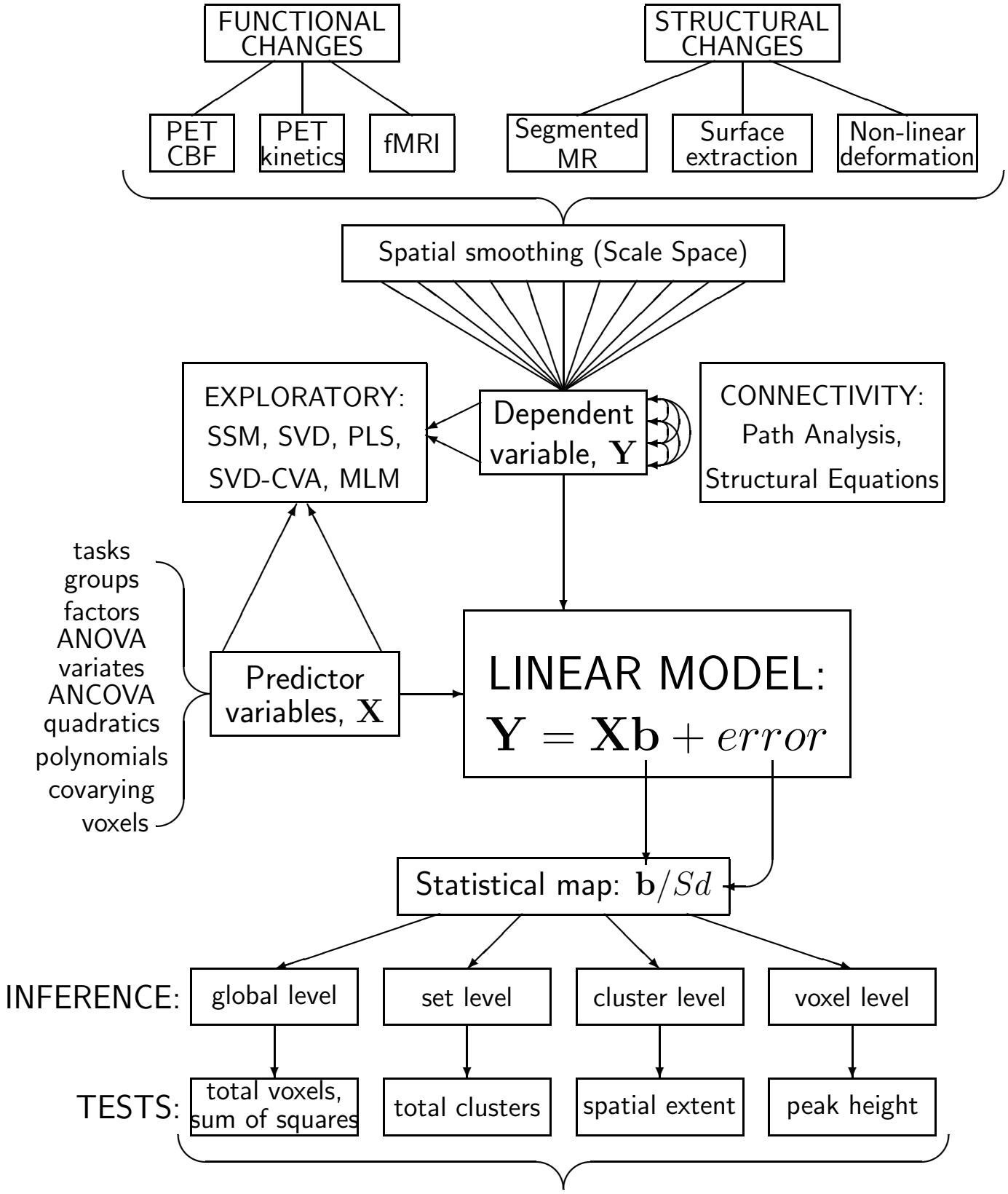

Table 2: Summary of canonical variables methods

SSM (Scaled Subprofile Model), Strother *et al.* (1995); SVD (Singular Value Decomp.), Friston *et al.* (1993): $\mathbf{Y} \approx \boxed{\mathbf{U'\Lambda V}}$
PLS (Partial Least Squares), McIntosh *et al.* (1996): $\boxed{\mathbf{X'Y}} \approx \boxed{\mathbf{U'\Lambda V}}$
Orthonormalised PLS: $(\mathbf{X'X})^{-1/2} \boxed{\mathbf{X'Y}} \approx \boxed{\mathbf{U'\Lambda V}}$
CVA (Canonical Variates Analysis): $(\mathbf{X'X})^{-1/2} \boxed{\mathbf{X'Y}} (\mathbf{Y'Y})^{-1/2} \approx \boxed{\mathbf{U'\Lambda V}}$
SVD-CVA, Friston *et al.* (1995c, 1996a): $\mathbf{Y} \approx \mathbf{U}^{*\prime}\mathbf{\Lambda}^{*}\mathbf{V}^{*}$, $\mathbf{Y}^{*} = \mathbf{Y}\mathbf{V}^{*\prime}$, $(\mathbf{X'X})^{-1/2} \boxed{\mathbf{X'Y}^{*}} (\mathbf{Y}^{*\prime}\mathbf{Y}^{*})^{-1/2} \approx \boxed{\mathbf{U'\Lambda V}}$
MLM (Multivariate Linear Models), Worsley *et al.* (1997): $\mathbf{Y} = \mathbf{Xb}+error, \quad \mathrm{Var}_{\mathrm{scans}}(\mathbf{Y}) = \mathbf{\Sigma}$, $(\mathbf{X'\Sigma X})^{-1/2} \boxed{\mathbf{X'Y}} = \mathrm{Var}(\mathbf{b})^{-1/2}\mathbf{b}$, $\approx \boxed{\mathbf{U'\Lambda V}}$